Identification of frequent activating *HER2* mutations in primary canine pulmonary adenocarcinoma

Gwendolen Lorch[1], Karthigayini Sivaprakasam[2], Victoria Zismann[2], Nieves Perdigones[2], Tania Contente-Cuomo[2], Alexandra Nazareno[2], Salvatore Facista[2], Shukmei Wong[2], Winnie S. Liang[2], Joseph M. Amann[3], Sara L. Sinicropi-Yao[3], Michael J. Koenig[3], Krista La Perle[4], Timothy G. Whitsett[2], Muhammed Murtaza[2], Jeffrey Trent[2], David P. Carbone[3], William P. D. Hendricks[2]

[1]Department of Veterinary Clinical Sciences, College of Veterinary Medicine, The Ohio State University, Columbus, Ohio, United States.

[2]Translational Genomics Research Institute, Phoenix, Arizona, United States.

[3]Department of Internal Medicine, James Thoracic Center, The Ohio State University, Columbus, Ohio, United States.

[4]Department of Veterinary Biosciences, Comparative Pathology & Mouse Phenotyping Shared Resource, College of Veterinary Medicine, The Ohio State University, Columbus, Ohio, United States.

Key Words: ERBB2, HER2, Lapatinib, Neratinib, Primary canine lung cancer, Naturally occurring canine cancer, Pulmonary adenocarcinoma, Pulmonary squamous cell carcinoma

ABSTRACT

Naturally occurring primary canine lung cancers are aggressive malignancies that are increasingly common in pet dogs. They share clinicopathologic features with human lung cancers in never-smokers, but their genetic underpinnings are unknown. Through multi-platform sequencing of 90 primary canine lung tumors or cell lines, we discovered somatic, coding *HER2 (ERRB2)* point mutations in 37% of canine pulmonary adenocarcinomas (cPAC, 28/76), but none in adenosquamous (cPASC, 0/11) or squamous cell (cPSCC, 0/3) carcinomas. In cPASC, *KRAS*, and *TP53* were the most frequently mutated genes (18% each). In cPSCC, no recurrently mutated

genes were identified, but individual somatic coding mutations were found in *BRAF* and *PTPN11*. In cPAC, we also identified recurrent somatic mutation of *TP53* (12%), *SMAD4* (5.3%), *PTEN* (5.3%), and *VHL* (4.0%). cPACs assessed by exome sequencing displayed a low mutation burden (median 64 SNVs, 19 CNVs and 1 SV). The majority (93%) of *HER2* mutations are hotspot V659E transmembrane domain (TMD) mutations comparable to activating mutations at this same site in human cancer. Other *HER2* mutations identified in this study were located in the extracellular and TMD. The *HER2* V659E mutation was detected in the plasma of 33% (2/6) of dogs with localized tumors bearing this mutation. HER2 V659E correlated with constitutive phosphorylation of Akt in cPAC cell lines and *HER2*^{V659E} lines displayed hypersensitivity to the HER2 inhibitors lapatinib and neratinib relative to *HER2* wild-type cell lines. These findings have immediate translational and comparative relevance for lung cancer and HER2 inhibition.

INTRODUCTION

Naturally occurring primary canine lung cancer is clinically challenging and increasingly common[1]. The disease course and underlying biology resemble that of human lung cancer in never-smokers which, in humans, accounts for 10-25% of lung cancers, causes approximately 26,000 deaths annually, and has a high incidence of erb-B family gene mutations such as those impacting *EGFR*. While incidence of smoking-related lung cancer is decreasing, lung cancer incidence in never-smokers is increasing[2]. Never-smoker lung cancer is primarily the non-small cell histology (NSCLC) arising from lung tissue as opposed to small cell (SCLC) arising in bronchi of smokers. NSCLC histologies include adenocarcinoma (AC) and squamous cell carcinoma (SCC). The etiology of never-smoker lung cancer is also distinct from smokers. It is associated with factors including environmental exposures (second-hand smoke, radon, asbestos, arsenic, silica, and pollution) as well as age, sex, family history, and genetic loci[3]. Unique genomic characteristics of human never-smoker lung cancer include low somatic mutation burden, enrichment for C:G>T:A transitions, and somatic activating point mutations or fusions impacting *EGFR* (45%), *ALK* (5-11%), *ROS* (1.5-6%), *HER2* (3-5%), and *RET* (2%)[4]. Five-year overall survival is estimated at 23%, but outcomes and treatment regimen are dependent on molecular subtype. For example, EGFR inhibitors can improve outcomes in *EGFR*-mutant lung cancers, however 85% of never-smoker lung AC and SCC cases are *EGFR* wild-type (WT) in

the United States. Clinical trials of immune checkpoint inhibitors have recently shown improved outcomes for human lung cancers, but analysis of large phase II immunotherapy trials suggests that benefits are limited in low-mutation-burden (≤ 10 mutations/Mb) cases such as those found in smokers[5]. A need exists for improved biologic understanding and development of new models to fuel translational research in never-smoker lung cancer.

Lung cancer in pet dogs has limited standard of care beyond surgery and little is known of its molecular underpinnings[1]. Primary lung tumors typically arise in older dogs (11 years) and resemble human NSCLC histotypes including canine pulmonary adenocarcinoma (cPAC), adenosquamous carcinoma (cPASC), and squamous cell carcinoma (cPSCC). These subtypes collectively represent 13-15% of primary lung tumors[6; 7]. Patients are often diagnosed late with lesions incidentally discovered during routine geriatric evaluation or due to nonspecific symptoms including dyspnea (6% to 24%) and cough (52% to 93%) that do not manifest until the tumor is more than 3 cm. These tumors can be diagnostically challenging. Rates at which ultrasound or CT-guided fine needle aspirates of the pulmonary mass provide cytologic diagnosis range from 38% to 90% of cases, varying broadly based on tumor accessibility and aspirate quality. At diagnosis, 71% of malignant canine lung tumors show signs of invasion and 23% show distant metastasis. Partial or complete lung lobectomy is standard of care, dependent on extent of disease spread. Median survival is 345 days for localized disease without nodal involvement where surgical remission can be achieved, but only 60 days when nodes are involved. Responses to cytotoxic chemotherapy (cisplatin, vindesine, doxorubicin, and mitoxantrone) in the setting of disseminated disease are limited. Targeted small molecules and immune checkpoint inhibitors have not been extensively studied in part because the molecular underpinnings of canine lung cancer remain largely unknown. Induced canine lung cancer models, such as purpose-bred beagles trained to smoke cigarettes or exposed to respirable aerosols of 239 plutonium ($^{239}PuO_2$) develop lung cancers, but do not recapitulate molecular features of human smoker lung cancer, showing only rare nuclear accumulation of p53, erb-B family overexpression, or *KRAS* hotspot mutation[6; 8; 9; 10]. In naturally occurring canine NSCLC, while comprehensive genomic profiling has been limited, *KRAS* hotspot mutation prevalence estimates from targeted studies have varied from 0-25%[7; 10; 11]. We have previously shown that EGFR mutation, overexpression, or phosphorylation is rare in cPAC compared to matched non-affected chemotherapy-naive lung tissue whereas significant over

expression and/or phosphorylation of PDGFRα, ALK, and HER2 are present[12]. We now describe for the first time the detailed genetic underpinnings of primary canine lung cancers through multi-platform next-generation sequencing of 90 cases.

MATERIALS AND METHODS

Sample Collection

90 previously untreated cases from the Comparative Oncology Genomics Consortium (CCOGC)[13] and The Ohio State University (OSU) College of Veterinary Medicine Biospecimen Repository were included. Veterinary pathologists board certified by the American College of Veterinary Pathologists (ACVP) confirmed tumor diagnosis based on histopathology. This study was approved by The OSU Institutional Animal Care Use Committee (2010A0015-R2). Tumor and normal tissue samples were flash frozen in liquid nitrogen or formalin-fixed and paraffin-embedded (FFPE). Cell lines were maintained in RPMI 1640 with GlutaMAX™ (Gibco™, Thermo Fisher Scientific #61870036) supplemented with 10% heat inactivated fetal bovine serum at 37ºC and 5% CO_2 and passaged at 90% confluence. Cell lines with known passage data (except BACA) were sequenced within the first eight passages of derivation and subsequently expanded for phenotypic studies. Canine cell lines were authenticated by IDEXX BioResearch (Columbia, MO) using Cell Check Canine STR Profile and Interspecies Contamination Tests on January 30, 2018 or by NkX2 (or TTF-1) RT-PCR. Human cell lines included BT474 (ATCC #HTB20, HER2 focal amplification) and H1781 (ATCC #CRL-5894, *HER2*^{G776V}). Whole blood was processed and stored within one hour of collection. Blood for cell-free DNA and germline DNA extraction was collected in 10ml K_2 EDTA Blood tubes (ThermoFisher Scientific #22-253-145). Plasma separation was performed at room temperature within 1h (2x serial centrifugation at 2000 rpm x 15 min). Plasma aliquots were stored frozen at -80°C. DNA extraction from plasma, white blood cells and tissue was performed with MagMAX Cell-Free DNA Isolation Kit (Thermo Fisher Scientific #A29319), DNeasy Blood and Tissue Kit (QIAGEN #69504) and Qiagen AllPrep DNA/RNA Mini Kit (QIAGEN #80204), respectively.

Exome Sequencing and Analysis

Informatic tools, versions, and flags are shown in **Table S1**. We utilized a custom Agilent SureSelect canine exome capture kit with 982,789 probes covering 19,459 genes. Exome libraries were sequenced on the Illumina HiSeq2000 producing paired end reads of 85bp. FASTQ files were aligned to the canine genome (CanFam3.1) using BWA v0.7.8. Aligned BAM files were realigned and recalibrated using GATK v3.3.0 and duplicate pairs were marked with Picard v1.128 (http://broadinstitute.github.io/picard). Somatic copy number variants (CNVs), and structural variants (SVs) were called with tCoNutT (https://github.com/tgen/tCoNuT) and DELLY v0.76 respectively. Somatic single nucleotide variants (SNV) were identified from two or more of the following callers: Seurat v2.6, Strelka v1.0.13 and MuTect v1.1.4. Germline SNVs were called using Haplotype Caller (GATK v3.3.0), Freebayes and samtools-Mpileup. Variant annotation was performed with SnpEff v3.5. The SomaticSignatures R package was used to identify mutation signatures.

Targeted Amplicon Sequencing and Analysis

We developed a custom canine cancer amplicon sequencing panel consisting of 250 amplicons targeting exons and hotspot regions in 51 genes, with amplicon sizes ranging from 91-271 bp. We pooled primers in two multiplexed pools to separate adjacent amplicons and any amplicons that showed cross-amplification using in silico PCR. We prepared sequencing libraries using droplet-based PCR amplification following the manufacturer's protocols for ThunderBolts Cancer Panel with specific modifications (RainDance Technologies), as previously described [[14]]. Sequencing was performed on Illumina MiSeq generating paired-end 275 bp reads. Sequencing reads were demultiplexed and extracted using Picardtools. Sequencing adapters were trimmed using ea-utils and fastq files were assessed for quality using FASTQC. Sequencing reads were aligned to CanFam3.1 using bwamem-MEM[15]. Custom in-house scripts based on samtools were used to create pileups for every sample. Pileups were analyzed in R to call SNVs and indels. For each potential non-reference allele at each targeted locus in a sample, we assessed the distribution of background noise across all other sequenced samples. To call a variant, we required the observed non-reference allele is an outlier from the background distribution with a Z-score > 5. In addition, we required tumor depth ≥100x, allele frequency ≥10%, number of reads supporting the variation ≥10, and allele fraction in the germline sample <1%. Finally, variant calls were manually curated by visualization in IGV v2.3.71.

Sanger Sequencing

23 primer pairs covering all exons of HER2 were designed using Primer 3 (http://bioinfo.ut.ee/primer3-0.4.0/) including a universal M13 tag. Amplicons were Sanger sequenced at the DNASU sequencing facility at Arizona State University on an ABI 3730XL (Applied Biosystems, Foster City, CA) and analyzed with Mutation Surveyor DNA Variant Analysis Software (SoftGenetics, State College, PA).

HER2 Inhibitor Drug Dose-Response Studies

HER2 inhibitors lapatinib (Selleckchem, #S2111) and neratinib (Puma Biotechnology, Los Angeles, CA), were assessed in 10-16 point 72 h drug-dose response screens (from $2x10^{-7}$ nM to 100 µM) with CellTiter-Glo® luminescent cell viability assay (Promega, #G7570). Cells were cultured in RPMI supplemented with 10% FBS and 1% Penicillin/Streptomycin. Luminescence was read using Synergy Mx (Biotek) plate reader. Six replicates were performed for each dose. Curve-fitting and IC_{50} calculations were performed using GraphPad Prism v7.00 (GraphPad Software, La Jolla, CA).

Droplet Digital PCR

HER2 V659E genotyping was performed on tumor samples and plasma cell-free DNA with droplet digital PCR (ddPCR). 50 µl reactions contained 2X KAPA PROBE FAST Master Mix (Kapa Biosystems, #KK4701), 200 µM dNTP Mix (New England BioLabs Inc, #N0477S), 1x Droplet Stabilizer (RainDance Technologies, #30-00826), 1 µM pooled primer mix (IDT), 1 µM mutant (FAM labeled) or wild type (TET labeled) *HER2* V659E probe (IDT), and 21.75 µL of template DNA. Each reaction was partitioned into 10 million droplets using the RainDrop Digital PCR Source instrument (RainDance). PCR amplification was performed as follows: 1 cycle 3 min at 95 °C, 50 cycles 15 sec at 95 °C and 1 min at 60 °C with a 0.5 °C/sec ramping from 95 °C to 60 °C, 1 cycle 98 °C for 10 min and hold at 4 °C. Droplet fluorescence was measured using RainDrop Digital PCR Sense instrument and analyzed using accompanying RainDrop Analyst II Software v.1.0 (RainDance). Primer and probe sequences used for *HER2* V659E detection in ctDNA were Forward: 5'-CCCACGACCACAGCCA-3', Reverse: 5'-CCCTGTGACATCCATCATTGC-3' and Probe: 5'-CAGAATGCCC(T/A)CCACAGC-3'.

qRT-PCR

cDNA was obtained by reverse transcription with iScript (Biorad, #1708891) and samples were subjected to HER2 (target) and HPRT1 (reference) amplification in a QuantStudio™ 6 Flex Real-Time PCR System under standard conditions with Syber Green technology (KapaBiosystems, #KK4602). Primer sequences were: HER2-Forward: 5'-CATCTGCACCATTGATGTCTA-3', HER2-Reverse: 5'-GGCCCAAGTCTTCATTCTGA-3', HPRT1-Forward: 5'GCAGCCCCAGCGTCGTGATT-3', HPRT1-Reverse: 5'CATCTCGAGCAAGCCGCTCAGT-3'. Data was analyzed with Quantstudio Real Time PCR software v1.1. Values for ΔCt, ΔΔCt, and fold changes were calculated as follows: ΔCt =Ct HER2 - Ct HPRT1; ΔΔCt= ΔCt tumor sample– ΔCt average of normal samples; and fold change =2^(- ΔΔCt).

Immunohistochemistry

HER2 protein expression was evaluated on FFPE sections (4 µm) of normal lung and tumor mounted on SuperFrost™ Plus glass slides (Fisher Scientific, #12-550-15). Slides were deparaffinized in xylene and rehydrated in an ethanol gradient. Antigen retrieval was performed with 1mM EDTA adjusted to pH 9.0. An autostainer (Dako, model S3400) was used to carry out immunostaining. A HER2 rabbit monoclonal antibody that detects the amino terminus of human HER2/ErbB2 (Cell Signaling Technology, #4290) was used at 1:400 in antibody diluent with background reducing components (Dako, #S3022) for 30 min. Slides were rinsed, incubated with secondary biotinylated rabbit anti-goat IgG (Vector Laboratories, BA-1000) diluted 1:200 in protein block for 30 min, rinsed, then incubated for 30 min in an avidin/biotin peroxidase system for detection of biotinylated antibodies (VECTASTAIN® Elite® ABC System, #PK-6100). IHC positive controls for HER2 tyrosine kinase receptor expression were single tissue samples of two canine complex mammary carcinomas[16]. Negative controls were performed on all tissues using a universal rabbit negative isotype control not directed against any known antigen (Dako, #IR600).

Quantitative Image Analysis

Immunostained and control 1x3-inch microscope slides were scanned at 40X on a high-resolution Scanscope XT (Leica Biosystems) at The Ohio State University Comparative Pathology & Mouse Phenotyping Shared Resource. For quantification of immunoreactivity, images were imported into Visiopharm Image Analysis software (Visiopharm, Hørsholm,

Denmark version 2017.27.0.3313), segmented into areas of tumor, necrosis, and normal lung tissue using color labels for each tissue type. HER2 connectivity was scored using the modified 10007 - HER2, Breast Cancer APP (Visiopharm). Thresholds were adjusted to match specimen HER2 stain intensities for accurate scoring. Area (μm^2) was quantified for each tissue type and percentages derived from specimen total tissue area. Tumor areas were further segmented into staining and non-staining categories. Percentages of stained and non-stained tumor were calculated based on total tumor area in μm^2. Maximum, mean, and minimum intensities were also quantified using a built-in software calculation. Staining is expressed as percentage of stain present with 100% equal to black (maximum dark brown) and 0% equal to white (no stain present). Initial thresholds and tissue types were established and mark-ups reviewed in consultation with a pathologist board-certified by the American College of Veterinary Pathologists to ensure accurate measurements and to differentiate between tissue types.

Immunoblot Analyses

Subconfluent cells were serum starved overnight, then treated with 20 nM neuregulin for 15 min prior to harvest. Cells were lysed in RIPA buffer (50 mM Tris, pH 8.0, 150 mM NaCl, 1% IGEPAL CA-630, 0.5% deoxycholate, 0.1% SDS) with cOmplete™ Mini Protease Inhibitor (Roche, #11836153001) and PhosSTOP™ (Roche, # 4906845001) and loaded in Laemmli buffer at 1 µg/µl. Samples were heated to 95°C for 5 min, then 25 µg were separated on 4-15% SDS-PAGE Criterion Gels (BioRad, #5671085) and transferred to Immobilon-FL PVDF membrane (MilliporeSigma, #IEVH7850). Membranes were dried for 1 hour to overnight, rehydrated in methanol, and washed. Membranes were blocked for 1 hour in LiCor blocking buffer (1% fish gelatin, 1x Tris Buffered Saline, pH 7.4, 0.02% sodium azide). Antibodies were diluted in primary antibody buffer (1% fish gelatin, 1x Tris Buffered Saline, pH 7.4, 0.1% Tween-20, 0.02% sodium azide) and added to the membranes for overnight incubation at 4°C. After washing, membranes were incubated for 1 h at room temperature with fluorescence-conjugated secondary antibodies conjugated in secondary antibody buffer (1% fish gelatin, 1x Tris Buffered Saline, pH7.4, 0.1 % Tween-20, 0.02% SDS, 0.02% sodium azide). After washing, membranes were scanned using the LiCor Odyssey CLx instrument. Primary antibodies were AKT (CST #4691S, 1:1000), phospho-AKT (CST #4060P, 1:1000), and β-actin (CST #4970S, 1:1000).

RESULTS AND DISCUSSION

The genomic landscape of naturally occurring primary canine lung cancer

In order to map the genomic landscape of canine lung cancer we undertook multi-platform next-generation sequencing of 90 NSCLC cases including 79 tumor/normal matched pairs and 11 cell lines (**Table 1**). The cohort included 76 cPAC, 11 cPASC, and 3 cPSCC. Labrador Retrievers represented the most commonly affected pure breed dog (21%) with mixed breeds (25%) and multiple other single pure breeds. The predominant cPAC subtype was papillary adenocarcinoma (62%). The cohort was gender-balanced (52% females) and primarily neutered/spayed (92%) with a median age at diagnosis of 11 years. Smoking status in the pet's household was not available. Extended clinical annotation is shown in **Table S2** and **Figure S1.**

To identify somatic point mutations, copy number changes, and translocations we first sequenced the coding genomic regions of five cPAC tumors and matching normal samples using a custom Agilent SureSelect canine exome capture kit comprising 982,789 probes covering 19,459 genes. Tumors were sequenced to mean target coverage of 298X with 99% of target bases covered ≥ 40X (**Table S3**). Germline samples were sequenced to mean target coverage of 263X with 99% of target bases covered ≥ 40X. A total of 648 high confidence somatic SNVs (median 64, range 37-406), 165 focal CNVs (median 19, range 0-116), and 3 SVs (median 1, range 0-1) were identified (**Tables S4-S6** and **Figure 1A)**. We identified non-recurrent, somatic SNVs in genes whose human orthologs have been implicated in human cancer according to COSMIC[17] Tiers 1 and 2 including nonsynonymous variants in *BCLAF1*, *CD274*, *CDH10*, *CSMD3*, *FANCD2*, *FOXP1*, *KIT*, *MAML3*, *NOTCH2*, *PER1*, *PTPN13*, *SEPT9* and *TP53*. CNVs in COSMIC genes included deletions in the tumor suppressors *CDKN2A/B* locus (40%) and *PTEN* (20% CNVs), as well as amplifications in the oncogenes *AKT1* (20%), *KIT* (20%) and *KDR* (20%) (**Figure 1B and Table S5**). The sole gene bearing recurrent nonsynonymous SNVs was *HER2* (80%) with the missense mutation V659E occurring in three cases and the missense mutation K676E in a fourth case (**Figure 1B**). No *HER2* amplifications were detected in these five tumors. We also assessed somatic point mutation signatures according to their trinucleotide context (**Figure S2**)[18; 19]. The most common signature in these five cases was COSMIC Signature 1A in 4/5 (80%) featuring frequent C>T substitutions at NpCpG trinucleotides. This signature is seen in 25/30 human cancer types, is associated with age, and is putatively the result of spontaneous deamination of 5-methyl-cytosine. COSMIC Signature 2 was also present in two cases, CCB050227 and OSU431895. This signature, characterized by C>T and C>G substitutions at

TpCpN, is associated with APOBEC cytidine deaminase activity, and though most prominent in cervical and bladder cancers, is found in 16 cancer types including lung adenocarcinoma and squamous cell carcinoma. No putatively pathogenic germline or somatic APOBEC mutations were observed in these five cases.

To identify somatic point mutations across a broader cohort of canine lung cancers, we used a custom canine cancer amplicon-based next generation sequencing panel to assess 250 coding regions (**Table S7**) of canine orthologs of 51 frequently mutated human cancer genes in 74 additional lung tumors (62 cPAC, 10 cPASC, 2 cPSCC) and two previously exome-sequenced tumors with matched normal as well as 10 cell lines (8 cPAC, 1 cPASC, and 1 cPSCC). These cases were sequenced to an average depth of 3,383x (**Table S8**). A median of 1 somatic coding point mutation (range 0-3) was identified across all cases. Likely pathogenic recurrent point mutations included *HER2* V659E (28%), *KRAS* G12D/V (3.3%), *SMAD4* D351Y/G (3.3%) and *TP53* R239Q/G (2.2%) (**Table S9**). The *TP53* R239Q/G mutation, previously described as rs851620436, is predicted to have a deleterious effect by SIFT[20] and, based on protein alignment, is equivalent to the human *TP53* codon R249, a hotspot bearing 739 mutations in COSMIC. *KRAS* mutations have been previously described in canine and human cancers, including lung cancer. The KRAS protein shares 100% identity between dog and human with the G12 codon within nucleotide binding domain being the most commonly mutated KRAS region. The SMAD4 protein shares 99% identity between dog and human with D351 in the MH2 domain being the 4th most commonly mutated codon with 45 mutations recorded in human lung cancer. Two additional somatic mutations were identified in single cases in *HER2* including A664T and K676E, (**Figure 1C**). Overall, recurrently mutated genes containing somatic potentially pathogenic SNVs included *TP53* (12.4%), *PTEN* (5.6%), *SMAD4* (4.4%), *KRAS* (4.4%), *VHL* (3.4%) and *HRAS* (2.2%). *TP53* missense and truncating mutations were comparable to DNA binding domain mutations seen in human *TP53*. *SMAD4* missense mutations were located in the MH2 human ortholog domain comparable to those recurrently described in human lung cancer. *KRAS* missense mutations were comparable to human *KRAS* mutations in codons G12 and Q61. Missense and truncating mutations in canine *PTEN* are distributed in the Phosphatase and C2 Tensin Type Domains of their human ortholog and comparable to truncated proteins described in human lung cancer (Q214*, L320*). Missense mutations in canine *HRAS* were located in codon Q61 in the GTPase domain comparable to the

established hotspot in human cancer. Finally, based on both exome and amplicon sequencing, we evaluated germline SNPs, finding putatively pathogenic germline variants in genes conferring susceptibility to lung cancer in humans and driver genes (*CHRNA3*, *DNAH11* and *ERBB2*, **Table S10**).

Squamous cell and adenosquamous carcinomas are under-studied entities, especially in non-smokers. This study includes 11 cPASC and 3 cPSCC tumors. In contrast with cPAC, no *HER2* mutations were identified in these tumors. *BRAF* and *PTPN11* mutations were only found in cPSCC cases and were the only recurrently mutated genes detected in this subtype. Environmental tobacco smoke (ETS) exposure was not recorded and second-hand smoke exposure remains possible. However, genomic landscapes of human lung cancers in never-smokers have not been shown to differ based on exposure to second-hand smoke[21].

***HER2* is frequently mutated in canine pulmonary adenocarcinoma (cPAC)**

HER2 was the most frequently mutated gene in our multi-platform cohort, occurring exclusively in cPACs (36.8%). V659E missense mutations located in the HER2 TMD occurred in 93.3% of *HER2*-mutant cases. Additional *HER2* mutations identified were A664T (OSU419040) and K676E (CCB050354). These mutations have not been previously described in orthologous regions of human *HER2*. *HER2* mutations were mutually exclusive with the only *EGFR* mutation detected in this cohort (the kinase domain mutation A726T) but did co-occur with mutations in *TP53*, *SMAD4*, *VHL*, *PTEN*, *AKT1* or *KDR*. *TP53* and *SMAD4* mutations were each found in 11% of the 27 HER2-mutant tumors, followed by *PTEN* 7% (2/27), *VHL*, *AKT* and *KDR* each accounting for 3% (1/27). Canine HER2 shares 92.2% amino acid identity with human HER2, with $HER2^{V659E}$ occurring at a highly conserved residue identical to the human variant (100% identity with human HER2 in the TMD from amino acids 654-674) and to the *neu* (rat HER2) variant identified in a rat glioblastoma cell line that originally led to discovery of *HER2*'s oncogene status[22]. *HER2* mutations have been identified as oncogenic drivers in approximately 1-4% of human NSCLC, mostly in exon 20, as a duplication or insertion coding for the amino acids YVMA at codon 776 resulting in constitutive HER2 kinase domain activation and downstream signaling through PI3K-AKT and MEK-ERK pathways[23; 24]. The patient population presenting with *HER2*-mutant NSCLC is predominately female never-smokers with adenocarcinoma histology who carry a median OS of ~2 years[24]. HER2 TMD

polar mutations (*HER2*$^{V659E/D}$, *HER2*^{G660D}) such as those we have discovered in cPAC are present in 0.18% of human lung adenocarcinomas overall, are exclusive with HER2 kinase domain mutations, can constitutively activate pro-survival HER2 signaling[25], and have been associated with responses to HER2 inhibitors[26]. While we did not sequence the full *HER2* gene in all cases, our amplicon analysis covers 7 of 27 exons of canine *HER2* (exon 8 and exons 17-22) including key transmembrane and kinase domains that, in humans, bear the majority of pathogenic mutations. Additionally, we performed Sanger sequencing of all exons in five canine cases (OSUK9PAD, BACA, CLAC, K9PADSQ and OSULSCC1) and found no additional somatic *HER2* mutations. It is nonetheless possible that somatic mutations occurring in other regions of *HER2* were not identified in amplicon-sequenced samples even though data facilitating functional interpretation of these variants would be limited.

***HER2* mutations are detectable in canine plasma DNA**

Cell-free tumor DNA (ctDNA) in plasma has been increasingly used for noninvasive genotyping in human cancer patients[27]. To develop a canine blood test that could rapidly identify dogs with lung cancer who carry the recurrent *HER2* mutation, we investigated whether cPAC *HER2* hotspot mutations are detectable in ctDNA. We evaluated plasma from 11 dogs, 5 with HER2-wild-type tumors and 6 with *HER2*^{V659E} tumors using droplet digital PCR (ddPCR) and custom primers targeting 57 bp surrounding codon 659 **(Table S11)**. We analyzed wild-type tumor samples, plasma DNA from unrelated commercially available canine plasma samples and template-free controls to establish assay specificity (BioreclamationIVT #BGLPLEDTA-100-P-m). Using uniform gating for all experiments, we found 1/7 template-free samples showed 1 wild-type droplet and no samples showed any evidence of mutant DNA amplification. In wild-type tumor and plasma DNA samples, 2/8 samples showed 1 mutant droplet each. Based on these results, we used required at least 3 mutant droplets to confidently detect *HER2*^{V659E}. We detected *HER2*^{V659E} in 6/6 positive control tumor DNA samples where we had previously identified V659E mutations using amplicon sequencing. In these samples, we observed a high correlation between allele fractions measured using amplicon sequencing and ddPCR (Pearson's r 0.976, p=0.0008). In 11 plasma samples from dogs with cPAC tested using ddPCR, median total cell-free DNA yield was 1.6 (range 0.3-10.0) (**Table S11**). Requiring at least 3 mutant droplets to support mutation detection, median limit of detection (LoD) for mutation allele fraction was calculated at 0.61% (range 0.10%-3.11%). *HER2*^{V659E} mutations were detected in

2/6 plasma samples from dogs with *HER2*^{V659E}-positive tumors at 1.9% and 2.3% allele fraction. Both ctDNA-positive cases had stage II cancer, consistent with low levels of ctDNA observed. *HER2*^{V659E} was not detected in any of plasma samples from dogs with HER2^{WT} tumors, confirming assay specificity (**Figure 1D)**.

HER2 expression in primary canine lung cancer

HER2 has been shown to bear activating point mutations, focal amplifications or copy number gains, and overexpression (by qRT-CPR and/or immunohistochemistry) in human cancers with amplifications. Overexpression typically occurs in a mutually exclusive fashion with point mutations. *HER2* amplification occurs in ~1% of human NSCLC (up to 12% of drug-resistant tumors)[28]. Protein overexpression has been reported to occur in a range from 6-35% of tumors including up to 42% of adenocarcinomas and has been shown to correlate with poor prognosis [29; 30; 31; 32]. In order to assess *HER2* copy number gains and overexpression, *HER2* copy number was first determined in the five exome-sequenced cases. No focal amplifications were detected (**Figure 1A**). However, these cases predominantly bore somatic putatively activating point mutations and might not be expected to also contain concomitant gains. Therefore, we evaluated HER2 RNA and protein expression by qRT-PCR and IHC. RNA samples from 45 lung tumors and 14 normal lung tissue samples not adjacent to tumor areas but from the same lung lobe were available for study. Median RNA HER2 fold change expression in normal lung samples was 1.06 (range 0.28-4.11) and 0.85 (range 0.07-4.50) in tumors. Fold changes over the median of normal were found in 31% of the tumors. Two adenocarcinoma samples had HER2 fold changes > 4 with respect to the median fold change for normals (CCB020293 and CCB050352).

To quantify HER2 protein expression in cPAC, digital image analysis was performed on eight tumors from FFPE surgical specimens. The histologic types evaluated for HER2 expression included three tubulopapillary and five papillary cPAC. Three of the samples bore the *HER2*^{V659E} hotspot mutations one bore *HER2*^{A664T} and four were *HER2*^{WT} according to amplicon and Sanger sequencing. All cases were positive for HER2, with homogeneous and diffuse staining of the tumor cell cytoplasm and cell membrane, but no staining in adjacent stroma or vasculature (**Figure S3**). Positive staining was observed in the bronchial epithelium of the adjacent non-affected lung in all cases. Consistent with absence of observed *HER2* amplifications, no

significant statistical differences as represented by mean ± SEM were detected in the tumor positivity percentage for HER2 (47±5.4 and 35±5.1) between the WT and *HER2* mutation groups, respectively. No significant differences in HER2 staining were present for either percent minimum (51±2.9 WT *vs.* 55±5.1, *HER2* mutations) or percent maximum (97±0.31 WT *vs.* 96±0.47 *HER2* mutations) stain intensity (**Table S12)**. Tumor RNA was available for two negative *HER2*^{V659E} samples (OSU421496, and OSU422025) to assess HER2 overexpression by qRT-PCR. HER2 expression fold changes were 1.10 (maximum and minimum percentage for tumor staining 97.30 and 47.34, respectively) and 3.01 (maximum and minimum percentage for tumor staining 97.40 and 59.06, respectively)

HER2 is constitutively active in *HER2*^{V659E} cPAC cell lines

HER2 V659E mutations have been shown to increase autophosphorylation and phosphorylation of EGFR, AKT, and mitogen-activated protein kinase when compared with WT *HER2* in humans[33]. *HER2* mutation status was determined in canine lung cancer cell lines by Sanger sequencing for the V659E amplicon in two cell lines (OSUK9PAPADRiley and OSUK9PAPADRex) which were positive for the mutation by ddPCR, in OSUK9PAPADOscar which was negative for the mutation, and for all *HER2* coding regions in five primary canine lung cancer cell lines: OSUK9PADSnickers, BACA, CLAC, OSUK9PADSQ and OSULSCC1. None of these cell lines bore additional mutations in *HER2*. We have previously shown that BACA and CLAC do not contain *HER2* amplification (by array comparative genomic hybridization) [34]. We next assessed HER2 activation in one *HER2*^{V659E} cPAC cell lines and three *HER2*^{WT} cell lines (two cPAC, papillary and unknown subtypes, and one cPASC) by Western blotting for total and phospho-AKT in the presence and absence of the ErbB ligand, neuregulin (hNRG) post-serum starvation. Only the *HER2*^{V659E} mutant line, OSUK9PADRex, showed constitutively high AKT phosphorylation post-starvation even in the absence of hNRG stimulation (**Figure 2A**).

***HER2*^{V659E} cPAC cell lines are hypersensitive to HER2 inhibitors**

Whereas *HER2*^{V659E} does not lead to increased levels of HER2 protein, the mutation is thought to stabilize receptor dimerization and constitutively activate downstream pro-survival signaling. Therefore anti-Her2 drugs (trastuzumab, neratinib, lapatinib, pertuzumab) offer a possibility of treatment for these patients. Herein we show that canine *HER2*^{V659E} cell lines are sensitive to the

small molecule HER2 inhibitors lapatinib and neratinib whereas *HER2*^{WT} cell lines are not. Four canine cell lines (one *HER2*^{V659E} and three *HER2*^{WT}), were initially treated with neratinib or lapatinib for 72h (**Figures 2B and S4**). Significant differences in viability were observed between mutant and WT cell lines for both drugs. The *HER2*-mutant cell line was more sensitive to both TK inhibitors than the rest of the cell lines (inhibitory concentration 50 (IC_{50}) < 200 nM in mutant versus IC_{50} > 2500 nM in HER2^{WT}). Furthermore, the OSUK9PAPADRex HER2^{V659E} cell line was seven times more sensitive to neratinib (IC_{50} = 25nM) than to lapatinib (IC_{50} = 168nM for lapatinib). In order to validate these findings, we tested neratinib response for 72h in 3 additional *HER2*-mutant cell lines. These included the human cell lines BT474, with known *HER2* amplification, and H1781, bearing a mutation in the kinase domain (HER2^{G776ins}), both of which are known to respond to HER2 inhibitors[33; 35]. They also included one canine cell line, OSUK9PAPADRiley *HER2*^{V659E}. Similar to previous results, all *HER2*^{V659E} cell lines were sensitive to neratinib with IC_{50} < 50nM. These studies confirm that *HER2*^{V659E} in cPAC is an activating event that may confer sensitivity to targeted HER2 inhibition.

Through multi-platform next-generation sequencing of 90 canine primary NSCLC (79 tumors and 11 cell lines), we have now characterized the genetic underpinnings of primary canine lung cancer. In cPAC, we have identified high frequency somatic hotspot mutations in the receptor tyrosine kinase HER2, a well-characterized human oncogene and drug target that is more commonly mutated in human never-smoker than smoker lung cancer[36]. We have additionally shown that these mutations can be detected in plasma, that they activate HER2 signaling, and that they confer sensitivity to small molecule HER2 inhibitors *in vitro*. Moreover, we have found recurrent *KRAS* and *TP53* mutations in cPASC and also provide a view of possible drivers in cPSCC. These data offer immediate diagnostic and therapeutic opportunities for dogs with primary lung cancer and aid comparative understanding of both never-smokers and also HER2-mutant lung cancer across species.

ACKNOWLEDGEMENTS

This study was supported by National Canine Cancer Foundation GL150H-005, the Bisgrove Scholars Program, philanthropic support to the TGen Foundation, CTSA UL1TR001070, NCI P30 CA016058, Brooke's Blossoming Hope, and the PetCo Foundation. We thank Drs. Alshad

Lalani, Irmina Diala, and Lisa Eli of Puma Biotechnology for fruitful discussion of HER2 inhibition and provision of neratinib for this study. We also thank Dr. Holly Borghese of the OSU CVM Veterinary Biospecimen Repository for her expertise in sample procurement and Dr. Kurtis Yearsley of the OSU Pathology Imaging Core for his expertise in quantitative image analysis.

AUTHOR CONTRIBUTIONS

Study conception and design: G.L, V.Z, J.T, D.P.C and W.H; Data acquisition: G.L, V.Z, T.C, S.F, S.W, W.S.L and N.P; Analysis and interpretation of data: G.L, K.S, V.Z, N.P, M.M, T.C, A.N, S.F, S.W, W.S.L, J.M.A, S.L.S, M.J.K, K.L.P, T.G.W, J.T, D.P.C, W.H; Drafting of manuscript: G.L, K.S, V.Z, N.P, W.H; Critical revision: G.L, K.S, V.Z, J.T, D.P.C, W.H.

COMPETING INTERESTS

WPDH has performed consulting work for The One Health Company, received research funding from Ethos Veterinary Health, and received travel support from Pathway Vet Alliance. WPDH, GL, and MM have filed a provisional patent (62/778,282) that describes these findings.

TABLES

Table 1. Genomic analyses performed in primary canine lung cancer.

Analysis platform	Samples analyzed*	Type of alteration detected
Exome	5 cPAC and matching normal	Germline and somatic SNVs, CNVs, and SVs
Amplicon	62 cPAC and matching normal, 8 cell lines	Germline and somatic SNVs and CNVs in 51 cancer genes
	10 cPASC and matching normal, 1 cell line	Germline and somatic SNVs and CNVs in 51 cancer genes
	2 cPSCC tumor and matching normal samples, 1 cell line	Germline and somatic SNVs and CNVs in 51 cancer genes
Total	**79 tumor-normal pairs, 10 cell lines**	

* an additional cell line (OSUK9PADRiley) was analyzed by sanger sequencing.
cPAC: Canine Pulmonary Adenocarcinoma; cPASC: Canine Pulmonary Adenosquamous Carcinoma;
cPSCC: Canine Squamous Cell Carcinoma.

FIGURES

Figure 1. The Genomic Landscape of Primary Canine Lung Cancers. (A) Somatic mutations identified by exome sequencing in matched tumor/normal tissue from five primary canine lung cancers. SV: structural variant, CNV: copy number variation, SNV: single nucleotide variant. (**B)** Recurrent likely pathogenic somatic mutations identified in primary canine lung cancers through multi-platform sequencing. CNVs were determined from tumor/normal exome data in five cPAC cases. SNVs were determined from combined tumor/normal exome and/or amplicon sequencing

across 89 total tumors and cell lines. (**C)** Distribution of somatic *HER2* mutations within the HER2 protein identified in primary canine lung cancers. The length of the lollipops is proportional to the number of mutations found. (**D)** Detection of *HER2* hotspot mutations in plasma of canine primary lung cancer patients.

Figure 2. *HER2*^{V659E} constitutively activates downstream HER2 signaling and is associated with response to HER2 inhibitors in primary canine pulmonary adenocarcinoma (cPAC) cell lines. (**A)** HER2 signaling activation in canine lung cancer cell lines. Phospho-Akt and Akt levels were assessed by Western blot under starvation both in the presence and absence of EGFR activation by hNRG in *HER2*^{V659E} and *HER2*^{WT} cPAC cell lines. (**B)** Neratinib drug-dose-response studies in primary lung cancer cell lines. Five canine cell lines (three HER2^{WT} and two HER2^{V659E}) and two human lung cancer positive controls with known HER2 activating mutations (BT474 – *HER2*-amplified, and H1781 – *HER2*^{G776V}) and HER inhibitor responses were treated with 14 neratinib doses ranging from 100 μM to 5.5x10^{-2} nM for 72 hours with CellTiterGlo viability endpoints. Survival is shown relative to DMSO vehicle control.

SUPPLEMENTAL TABLES AND FIGURES

Table S1. Informatic tools utilized in primary canine lung cancer genomic analyses.

Table S2. Extended clinical and multiplatform annotation of primary canine lung cancer cases.

Table S3. Sequencing metrics for primary canine lung cancer exome analysis.

Table S4. Somatic coding SNVs identified by exome sequencing of primary canine lung cancers.

Table S5. Somatic coding CNVs identified by exome sequencing of primary canine lung cancers.

Table S6. Somatic coding SVs identified by exome sequencing of primary canine lung cancers.

Table S7. Canine genomic regions covered by custom amplicon panel.

Table S8. Sequencing metrics for primary canine lung cancer amplicon analysis.

Table S9. Somatic coding SNVs identified by panel sequencing of primary canine lung cancers.

Table S10. Germline SNPs in COSMIC Tier 1 cancer genes identified by exome and panel sequencing in primary canine lung cancers.

Table S11. Non-invasive detection of *HER2*^{V659E} in the plasma of primary canine lung cancer patients.

Table S12. HER2 protein expression and quantification by immunohistochemistry.

Figure S1. Extended clinical annotation of primary canine lung cancer patients. (**A**) Distribution of affected breeds. (**B**) Age at diagnosis. (**C**) Primary tumor location distribution. (**D**) Sex distribution. (**E**) Adenocarcinoma subtype distribution. (**F**) Treatment. Yr= years.

Figure S2. Somatic mutation signatures identified by exome sequencing in primary canine lung cancers. (**A**) The distribution of somatic single nucleotide mutation types in their trinucleotide context from tumor/normal exome sequencing of five cPAC cases. (**B**) The most common mutation signatures based on trinucleotide context and frequency of somatic single nucleotide mutations from tumor/normal exome sequencing of five cPAC cases. COSMIC Signature 1A (C>T substitutions at NpCpG trinucleotides that are associated with age) was present in four cases. COSMIC Signature 2 (C>T and C>G substitutions at TpCpN, associated with APOBEC cytidine deaminase activity) was present in two cases.

Figure S3. HER2 cellular location and function in primary canine lung cancer. (A) Canine papillary adenocarcinoma with intense, complete, circumferential membrane (white arrow) and lateral cytoplasmic membrane (black arrow) anti-HER2 antibody positive staining (brown) in a patient with wild-type HER2. (**B**) Canine papillary adenocarcinoma with moderate cytoplasmic (black arrow) anti-HER2 antibody positive staining (light brown) in a patient with wild-type HER2. x 40; bar 50 µm. (**C**) Anti-HER2 immunohistochemistry of a Grade 1 canine papillary adenocarcinoma wild type for HER2. x 20. (**D**) Segmentation mark-up of the tumor from adjacent normal lung. Tumor is identified by green, whereas red is area within tumor that contains no tissue, and yellow represents areas of non-tumor such as necrosis or tumor stroma. x20.

Figure S4. Canine lung cancer cell line sensitivity to lapatinib. Four canine cell lines (three *HER2*^{WT} and one *HER2*^{V659E}) were treated with 14 lapatinib doses ranging from 100 μM to $5.5x10^{-2}$nM for 72 hours. CellTiterGlo viability endpoints were measured and shown as the percent survival relative to DMSO vehicle control.

REFERENCES

[1]D.W. Wilson, Tumors of the Respiratory Tract, in: D.J. Meuten, (Ed.), Tumors in domestic animals, John Wiley & Sons, 2017, pp. 467-498.

[2]C. Clément-Duchêne, H. Wakelee, Lung Cancer Incidence in Never Smokers. European Journal of Clinical & Medical Oncology 2 (2010).

[3]J.M. Samet, E. Avila-Tang, P. Boffetta, L.M. Hannan, S. Olivo-Marston, M.J. Thun, C.M. Rudin, Lung cancer in never smokers: clinical epidemiology and environmental risk factors. Clin Cancer Res 15 (2009) 5626-5645.

[4]R. Govindan, L. Ding, M. Griffith, J. Subramanian, N.D. Dees, K.L. Kanchi, C.A. Maher, R. Fulton, L. Fulton, J. Wallis, K. Chen, J. Walker, S. McDonald, R. Bose, D. Ornitz, D. Xiong, M. You, D.J. Dooling, M. Watson, E.R. Mardis, R.K. Wilson, Genomic landscape of non-small cell lung cancer in smokers and never-smokers. Cell 150 (2012) 1121-1134.

[5]M.D. Hellmann, T.E. Ciuleanu, A. Pluzanski, J.S. Lee, G.A. Otterson, C. Audigier-Valette, E. Minenza, H. Linardou, S. Burgers, P. Salman, H. Borghaei, S.S. Ramalingam, J. Brahmer, M. Reck, K.J. O'Byrne, W.J. Geese, G. Green, H. Chang, J. Szustakowski, P. Bhagavatheeswaran, D. Healey, Y. Fu, F. Nathan, L. Paz-Ares, Nivolumab plus Ipilimumab in Lung Cancer with a High Tumor Mutational Burden. N Engl J Med 378 (2018) 2093-2104.

[6]F.F. Hahn, Muggenburg B.A., Griffith W.C., , (Ed.) Primary lung cacer in the longevity study/control population of the ITRI beagle dog colony., National Technical Information Service, Springfield, VA, 1992.

[7]S.M. Griffey, S.A. Kraegel, B.R. Madewell, Rapid detection of K-ras gene mutations in canine lung cancer using single-strand conformational polymorphism analysis. Carcinogenesis 19 (1998) 959-963.

[8]O. Auerbach, E.C. Hammond, D. Kirman, L. Garfinkel, Effects of cigarette smoking on dogs. II. Pulmonary neoplasms. Arch Environ Health 21 (1970) 754-768.

[9]F.C. Leung, L.R. Bohn, G.E. Dagle, Elevated epidermal growth factor receptor binding in plutonium-induced lung tumors from dogs. Proc Soc Exp Biol Med 196 (1991) 385-389.

[10]L.A. Tierney, F.F. Hahn, J.F. Lechner, p53, erbB-2 and K-ras gene alterations are rare in spontaneous and plutonium-239-induced canine lung neoplasia. Radiation Research 145 (1996) 181-187.

[11]S.A. Kraegel, P.H. Gumerlock, D.L. Dungworth, V.I. Oreffo, B.R. Madewell, K-ras activation in non-small cell lung cancer in the dog. Cancer Research 52 (1992) 4724-4727.

[12]E.T. Mariotti, C. Premanandan, G. Lorch, Canine pulmonary adenocarcinoma tyrosine kinase receptor expression and phosphorylation. BMC veterinary research 10 (2014) 19.

[13]I. Gordon, M. Paoloni, C. Mazcko, C. Khanna, The Comparative Oncology Trials Consortium: using spontaneously occurring cancers in dogs to inform the cancer drug development pathway. PLoS medicine 6 (2009) e1000161.

[14]D.S. Murtaza M, Pogrebniak K, Rueda OM, Provenzano E, Grant J, Chin SF, Tsui DW, Marass F, Gale D, Ali HR, Shah P, Contente-Cuomo T, Farahani H, Shumansky K, Kingsbury Z, Humphray S, Bentley D, Shah SP, Wallis M, Rosenfeld N, Caldas C, Multifocal clonal evolution characterized using circulating tumour DNA in a case of metastatic breast cancer. Nat Commun 4 (2015) 8760.

[15]H. Li, B. Handsaker, A. Wysoker, T. Fennell, J. Ruan, N. Homer, G. Marth, G. Abecasis, R. Durbin, S. Genome Project Data Processing, The Sequence Alignment/Map format and SAMtools. Bioinformatics 25 (2009) 2078-2079.

[16]W.L. Hsu, H.M. Huang, J.W. Liao, M.L. Wong, S.C. Chang, Increased survival in dogs with malignant mammary tumours overexpressing HER-2 protein and detection of a silent single nucleotide polymorphism in the canine HER-2 gene. Veterinary Journal 180 (2009) 116-123.

[17]S.A. Forbes, D. Beare, H. Boutselakis, S. Bamford, N. Bindal, J. Tate, C.G. Cole, S. Ward, E. Dawson, L. Ponting, R. Stefancsik, B. Harsha, C.Y. Kok, M. Jia, H. Jubb, Z. Sondka, S. Thompson, T. De, P.J. Campbell, COSMIC: somatic cancer genetics at high-resolution. Nucleic Acids Res 45 (2017) D777-D783.

[18]L.B. Alexandrov, S. Nik-Zainal, D.C. Wedge, S.A. Aparicio, S. Behjati, A.V. Biankin, G.R. Bignell, N. Bolli, A. Borg, A.-L. Børresen-Dale, Signatures of mutational processes in human cancer. Nature 500 (2013) 415.

[19]J.S. Gehring, B. Fischer, M. Lawrence, W. Huber, SomaticSignatures: inferring mutational signatures from single-nucleotide variants. Bioinformatics 31 (2015) 3673-3675.

[20]P. Kumar, S. Henikoff, P.C. Ng, Predicting the effects of coding non-synonymous variants on protein function using the SIFT algorithm. Nat Protoc 4 (2009) 1073-1081.

[21]S. Couraud, D. Debieuvre, L. Moreau, P. Dumont, J. Margery, E. Quoix, B. Duvert, L. Cellerin, N. Baize, B. Taviot, M. Coudurier, J. Cadranel, P. Missy, F. Morin, J.F. Mornex, G. Zalcman, P.J. Souquet, C.I.-s.i. Bio, No impact of passive smoke on the somatic profile of lung cancers in never-smokers. Eur Respir J 45 (2015) 1415-1425.

[22]C.I. Bargmann, M.C. Hung, R.A. Weinberg, Multiple independent activations of the neu oncogene by a point mutation altering the transmembrane domain of p185. Cell 45 (1986) 649-657.

[23]J. Mazieres, S. Peters, B. Lepage, A.B. Cortot, F. Barlesi, M. Beau-Faller, B. Besse, H. Blons, A. Mansuet-Lupo, T. Urban, D. Moro-Sibilot, E. Dansin, C. Chouaid, M. Wislez, J. Diebold, E. Felip, I. Rouquette, J.D. Milia, O. Gautschi, Lung cancer that harbors an HER2 mutation: epidemiologic characteristics and therapeutic perspectives. J Clin Oncol 31 (2013) 1997-2003.

[24]J. Mazieres, F. Barlesi, T. Filleron, B. Besse, I. Monnet, M. Beau-Faller, S. Peters, E. Dansin, M. Fruh, M. Pless, R. Rosell, M. Wislez, P. Fournel, V. Westeel, F. Cappuzzo, A. Cortot, D. Moro-Sibilot, J. Milia, O. Gautschi, Lung cancer patients with HER2 mutations treated with chemotherapy and HER2-targeted drugs: results from the European EUHER2 cohort. Ann Oncol 27 (2016) 281-286.

[25]T.T.N. Kanika Bajaj Pahuja, Bijay S. Jaiswal, Kumar Prabhash, Tarjani M. Thaker,, S.C. Kate Senger, Noelyn M. Kljavin, Aju Antony, Sameer Phalke, Prasanna Kumar, Marco Mravic, Eric W. Stawiski, Derek Vargas, Steffen Durinck, Ravi Gupta, Arati Khanna-Gupta, Sally E. Trabucco, Ethan S. Sokol, Ryan J. Hartmaier, Ashish Singh, Anuradha Chougule, Vaishakhi Trivedi, Amit Dutt, Vijay Patil, Amit Joshi, Vanita Noronha, James Ziai, Sripad D. Banavali, Vedam Ramprasad, William F. DeGrado, Raphael Bueno,

Natalia Jura, and Somasekar Seshagiri, Actionable Activating Oncogenic ERRB2/HER2 Transmembrane and Juxtamembrane DomainMutations. Cancer Cell (2018) 15.

[26]S.I. Ou, A.B. Schrock, E.V. Bocharov, S.J. Klempner, C.K. Haddad, G. Steinecker, M. Johnson, B.J. Gitlitz, J. Chung, P.V. Campregher, J.S. Ross, P.J. Stephens, V.A. Miller, J.H. Suh, S.M. Ali, V. Velcheti, HER2 Transmembrane Domain (TMD) Mutations (V659/G660) That Stabilize Homo- and Heterodimerization Are Rare Oncogenic Drivers in Lung Adenocarcinoma That Respond to Afatinib. J Thorac Oncol 12 (2017) 446-457.

[27]N. Perdigones, M. Murtaza, Capturing tumor heterogeneity and clonal evolution in solid cancers using circulating tumor DNA analysis. Pharmacol Ther 174 (2017) 22-26.

[28]K. Takezawa, V. Pirazzoli, M.E. Arcila, C.A. Nebhan, X. Song, E. de Stanchina, K. Ohashi, Y.Y. Janjigian, P.J. Spitzler, M.A. Melnick, HER2 amplification: a potential mechanism of acquired resistance to EGFR inhibition in EGFR-mutant lung cancers that lack the second-site EGFRT790M mutation. Cancer discovery (2012).

[29]I. Rouquette, V. Lauwers-Cances, C. Allera, L. Brouchet, J. Milia, Y. Nicaise, J. Laurent, M.-B. Delisle, G. Favre, A. Didier, Characteristics of lung cancer in women: importance of hormonal and growth factors. Lung Cancer 76 (2012) 280-285.

[30]C. Pellegrini, M. Falleni, A. Marchetti, B. Cassani, M. Miozzo, F. Buttitta, M. Roncalli, G. Coggi, S. Bosari, HER-2/Neu alterations in non-small cell lung cancer: a comprehensive evaluation by real time reverse transcription-PCR, fluorescence in situ hybridization, and immunohistochemistry. Clinical cancer research 9 (2003) 3645-3652.

[31]C.J. Langer, P. Stephenson, A. Thor, M. Vangel, D.H. Johnson, Trastuzumab in the treatment of advanced non-small-cell lung cancer: is there a role? Focus on Eastern Cooperative Oncology Group study 2598. Journal of clinical oncology 22 (2004) 1180-1187.

[32]P.N. Lara Jr, L. Laptalo, J. Longmate, D.H. Lau, R. Gandour-Edwards, P.H. Gumerlock, J.H. Doroshow, D.R. Gandara, Trastuzumab plus Docetaxel in HER2/neu–Positive Non–Small-Cell Lung Cancer: A California Cancer Consortium Screening and Phase II Trial. Clinical lung cancer 5 (2004) 231-236.

[33]K. Suzawa, S. Toyooka, M. Sakaguchi, M. Morita, H. Yamamoto, S. Tomida, T. Ohtsuka, M. Watanabe, S. Hashida, Y. Maki, J. Soh, H. Asano, K. Tsukuda, S. Miyoshi, Antitumor

effect of afatinib, as a human epidermal growth factor receptor 2-targeted therapy, in lung cancers harboring HER2 oncogene alterations. Cancer Sci 107 (2016) 45-52.

[34]F. Clemente-Vicario, C.E. Alvarez, J.L. Rowell, S. Roy, C.A. London, W.C. Kisseberth, G. Lorch, Human genetic relevance and potent antitumor activity of heat shock protein 90 inhibition in canine lung adenocarcinoma cell lines. PloS one 10 (2015) e0142007.

[35]A. Canonici, M. Gijsen, M. Mullooly, R. Bennett, N. Bouguern, K. Pedersen, N.A. O'Brien, I. Roxanis, J.-L. Li, E. Bridge, Neratinib overcomes trastuzumab resistance in HER2 amplified breast cancer. Oncotarget 4 (2013) 1592.

[36]H. Shigematsu, T. Takahashi, M. Nomura, K. Majmudar, M. Suzuki, H. Lee, I.I. Wistuba, K.M. Fong, S. Toyooka, N. Shimizu, Somatic mutations of the HER2 kinase domain in lung adenocarcinomas. Cancer Research 65 (2005) 1642-1646.

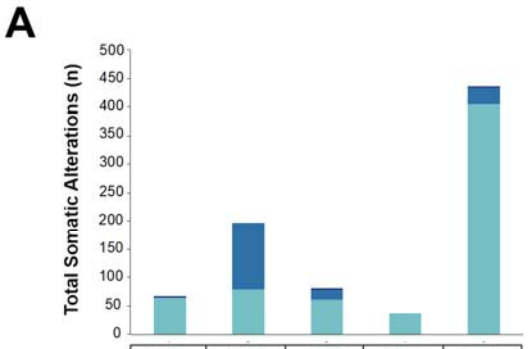

	CCB 010387	CCB 050227	CCB 050354	OSU 396622	OSU 431895
SV	1	0	1	0	1
CNV	2	116	23	0	34
SNV	64	80	61	37	406

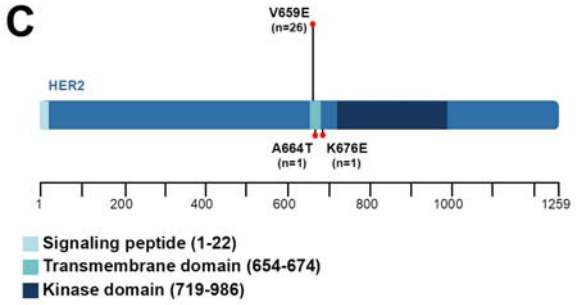

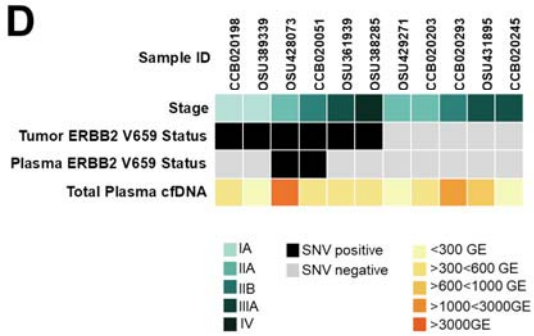

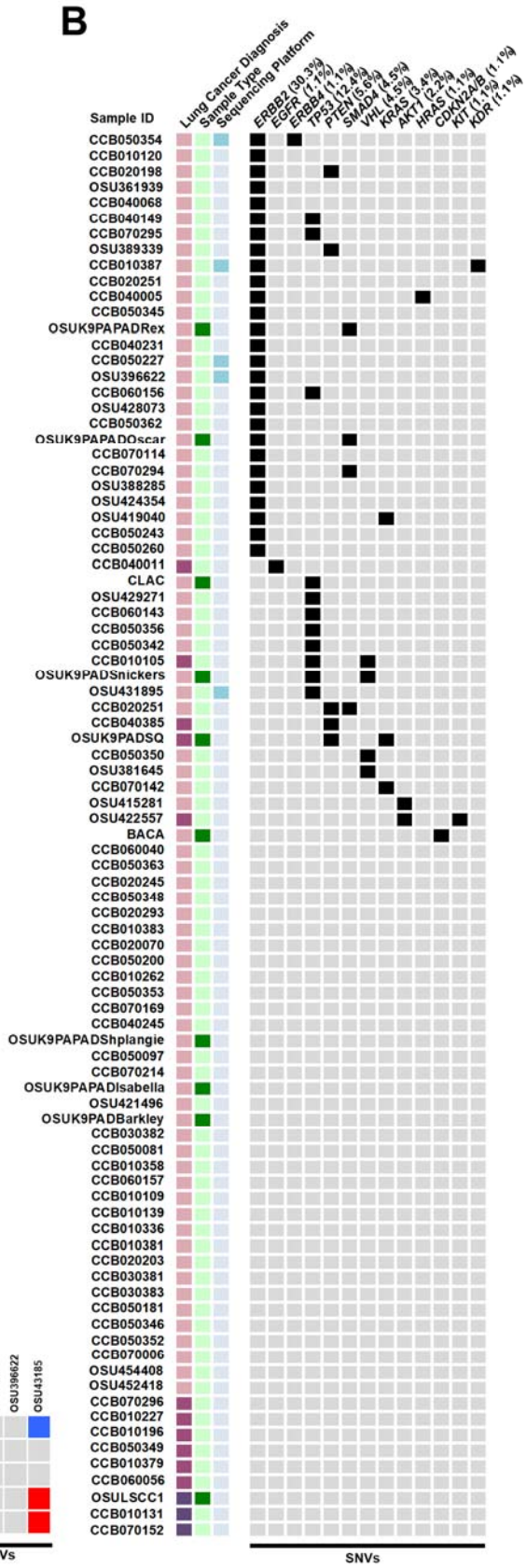

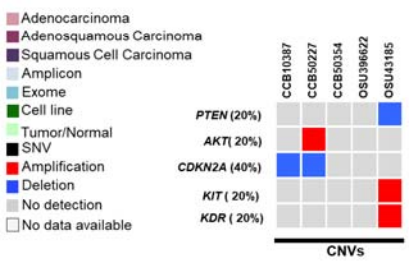

Figure 1. The Genomic Landscape of Primary Canine Lung Cancers. (A) Somatic mutations identified by exome sequencing in matched tumor/normal tissue from five primary canine lung cancers. SV: structural variant, CNV: copy number variation, SNV: single nucleotide variant. (**B)** Recurrent likely pathogenic somatic mutations identified in primary canine lung cancers through multi-platform sequencing. CNVs were determined from tumor/normal exome data in five cPAC cases. SNVs were determined from combined tumor/normal exome and/or amplicon sequencing across 89 total tumors and cell lines. (**C)** Distribution of somatic *HER2* mutations within the HER2 protein identified in primary canine lung cancers. The length of the lollipops is proportional to the number of mutations found. (**D)** Detection of *HER2* hotspot mutations in plasma of canine primary lung cancer patients.

A

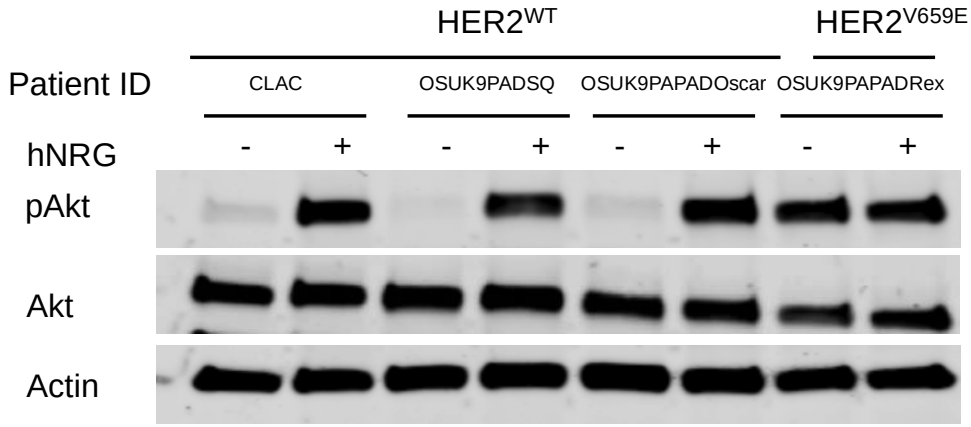

B

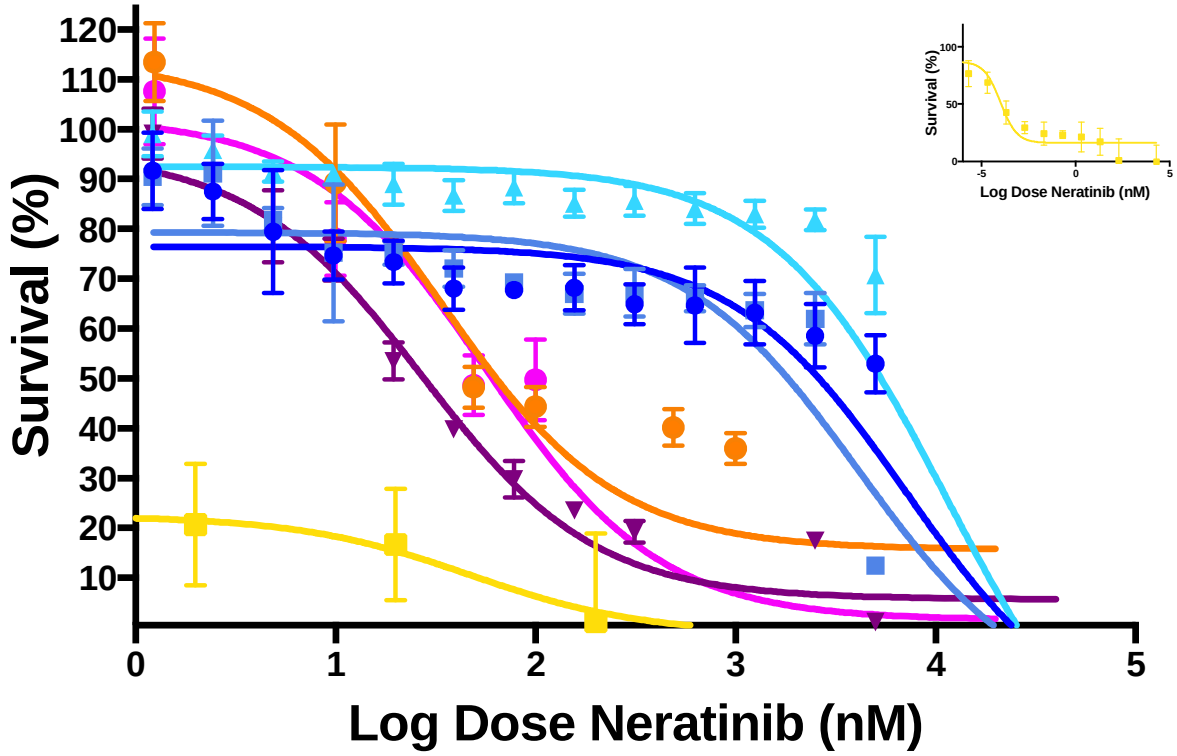

- BACA (HER2^{WT})
- OSUK9PADSnickers (HER2^{WT})
- OSUK9PAPADOscar (HER2^{WT})
- OSUK9PAPADRex (HER2^{V659E})
- OSUK9PAPADRiley (HER2^{V659E})
- H1781 (HER2^{G776ins})
- BT474 (HER2^{amp})

Sample	IC50 (nM)
BACA	7140
OSUK9PADSnickers	4136
OSUK9PAPADOscar	11385
OSUK9PAPADRex	23.13
OSUK9PAPADRiley	48.45
H1781	35.38
BT474	0.00010

Figure 2. *HER2*^{V659E} constitutively activates downstream HER2 signaling and is associated with response to HER2 inhibitors in primary canine pulmonary adenocarcinoma (cPAC) cell lines. (**A)** HER2 signaling activation in canine lung cancer cell lines. Phospho-Akt and Akt levels were assessed by Western blot under starvation both in the presence and absence of EGFR activation by hNRG in *HER2*^{V659E} and *HER2*^{WT} cPAC cell lines. (**B)** Neratinib drug-dose-response studies in primary lung cancer cell lines. Five canine cell lines (three HER2^{WT} and two HER2^{V659E}) and two human lung cancer positive controls with known HER2 activating mutations (BT474 – *HER2*-amplified, and H1781 – *HER2*^{G776V}) and HER inhibitor responses were treated with 14 neratinib doses ranging from 100 μM to 5.5×10^{-2} nM for 72 hours with CellTiterGlo viability endpoints. Survival is shown relative to DMSO vehicle control.